

**P2.5 SIMULATION OF ARCTIC CLOUD PROPERTIES DURING THE SPRING SEASON OF SHEBA/FIRE-ACE EXPERIMENT USING A STATISTICAL CLOUD SCHEME IN THE CCCMA SINGLE-COLUMN MODEL**

Junhua Zhang\* and Ulrike Lohmann  
Department of Physics and Atmospheric Science, Dalhousie University, Halifax,  
Nova Scotia, Canada

**1. INTRODUCTION**

Intercomparison of global climate model simulations showed large discrepancies in prediction of present and future climate in the Arctic (e.g., Randall et al. 1998). The important role of Arctic on climate and the uncertainty and difficulty in the climate model simulation motivated the Surface Heat Budget of the Arctic Ocean (SHEBA) experiment [Uttal et al. 2002] to set a ship adrift through the Arctic sea ice for one year from Nov. 1997 - Oct. 1998. The FIRE Arctic Clouds Experiments (FIRE. ACE) took place during part of the SHEBA year from April - July 1998 [Curry et al. 2000].

Spring is the transition season in the Arctic. Mixed-phase clouds often occur in this region [Curry et al. 1996, Shupe et al. 2001]. Curry et al [2000] showed that simulations with three large scale single column models (SCMs) for May 1998 of the SHEBA/FIRE. ACE experiment underestimated the column liquid water path and low cloud amount which is partly due to inaccurately representing the mixed-phase clouds. One of the main goals of the SHEBA/FIRE. ACE experiment is to improve the ice or mixed cloud microphysical parameterization. In this study, the Canadian single column model is used to simulate the cloud properties during the SHEBA/FIRE. ACE experiment in April 1998.

**2. OBSERVED CLOUDS PROPERTIES**

The cloud properties studied here are the cloud cover fraction (CF), liquid water path (LWP), ice water path (IWP), liquid water fraction (LF), and precipitation during the SHEBA/FIRE-ACE experiment. Cloud cover is measured by an 8mm cloud radar [Intrieri et al. 2002]. Plate 1 is the time-height plot of radar observed cloud cover

frequency during April. Most of the time this area is covered by cloud from surface till to the altitude as high as 9 km. Figure 1 is the ice water path retrieved from radar observation depending on an empirical retrieval method [Shupe et al., 2001] and liquid water path retrieved from the Microwave Radiometer measurements [Lin et al. 2001]. It shows that liquid, ice and mixed-phase cloud occurs frequently during the month. Figure 2 is the liquid water fraction obtained from the 18 in-situ flights measurement in April [Korolev et al. 1999]. It shows that mixed-phase clouds often occur between 252 K and 270K. Liquid clouds can exist at temperature as low as 252 K and ice clouds occur at temperatures around 270K are not uncommon. Hourly mean precipitation data are from a snow gauge system [Persson et al., 2002].

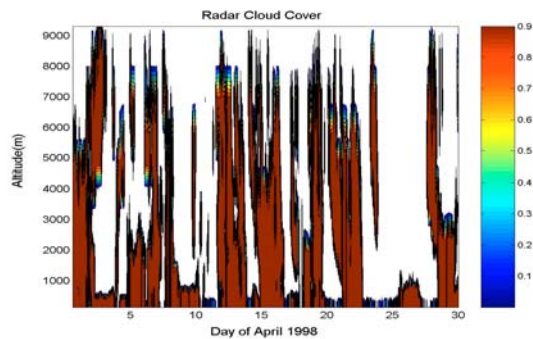


Plate 1 Cloud cover observed by cloud radar

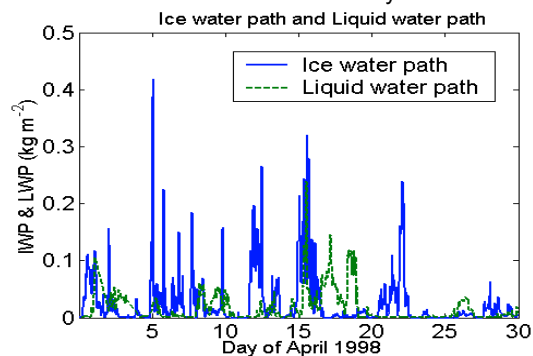


Figure 1 Observed Ice Water Path and Liquid Water Path by radar and Microwave Radiometer

\* Corresponding author address: Junhua Zhang, Dept. of Physics and Atmospheric Science, Dalhousie Univ., Halifax, N.S., B3H 3J5, Canada; e-mail: zhang@mathstat.dal.ca

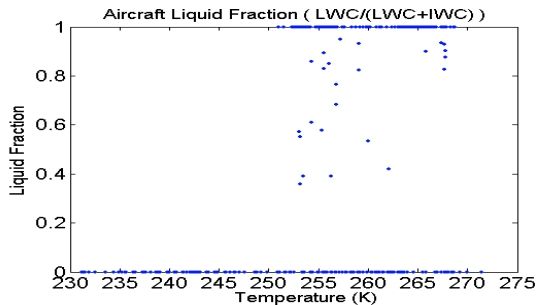


Figure 2 Observed liquid water fraction by aircraft

### 3. MODEL SIMULATION

#### 3.1 SIMULATION WITH THE ORIGINAL MODEL SETUP

The SCM we used is the Canadian Centre for Climate Modelling and Analysis (CCCMA) SCM. The prognostic variables of the CCCMA SCM are temperature, water vapor and the number concentration and mass mixing ratio of cloud liquid water and cloud ice [Lohmann et al, 1999]. Fractional cloud cover and cloud water content are diagnostically calculated by a statistical cloud scheme following the ideas of Sommeria and Dearnorff [1977]. The threshold relative humidity is set to  $RH_c=85\%$  to calculate the standard deviation of the distribution function [Smith, 1990]. Ice crystals can form by heterogeneous freezing of cloud droplet between  $-35^{\circ}\text{C}$  and  $-0^{\circ}\text{C}$ . Below  $-35^{\circ}\text{C}$ , all cloud droplets freeze within one time step. If the ice water content exceeds a threshold,  $IWC_{crit}=10$  mg/kg for the original set up, the Bergeron-Findeisen process leads to a glaciation of the supercooled cloud.

The SCM is initialized by the reanalysis data of the European Center for Medium Range Weather Forecasts (ECMWF) [Bretherton et al., 2002]. Temperature and specific humidity are nudged towards ECMWF data using a relaxation time step determined by the grid length scale and average wind speed in the region [Ghan et al., 2000]. Plate 2 shows the simulated cloud cover with the original model setup. Much fewer clouds are predicted by SCM as compared to the radar observation and no cloud exists between 3000m and 5000m. Figure 3 shows that the ice water path is much smaller than the observation during the whole month. As shown in figure 4, the simulated liquid/mixed phase cloud mainly occurs between April 15 -April 20. The model predicts more liquid water than observed during this period. Although the simulated liquid water fraction agrees well with the aircraft observation as shown in figure 5, the

lowest temperature at which the mixed clouds occur is about 245K, 7K lower than observed 252K.

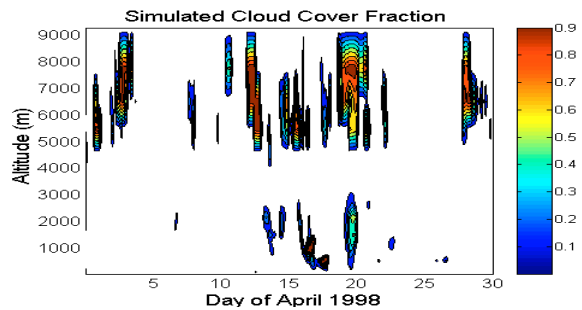


Plate 2 Cloud cover simulated by the original model setup

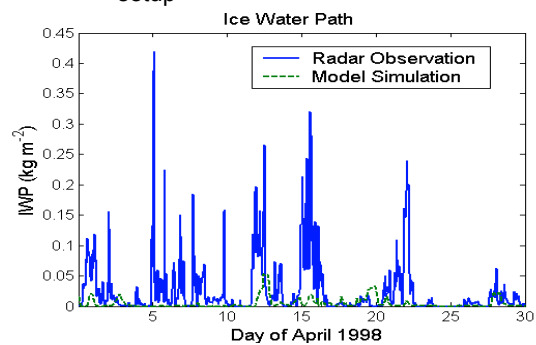


Figure 3 Comparison of ice water path

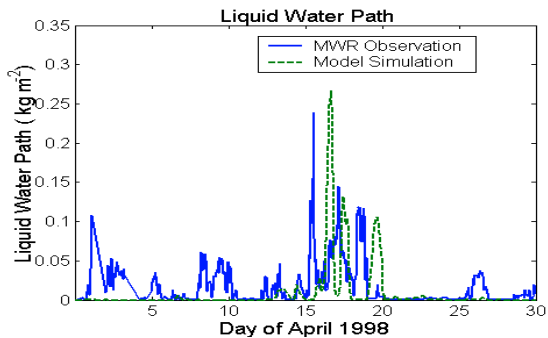


Figure 4 Comparison of liquid water path

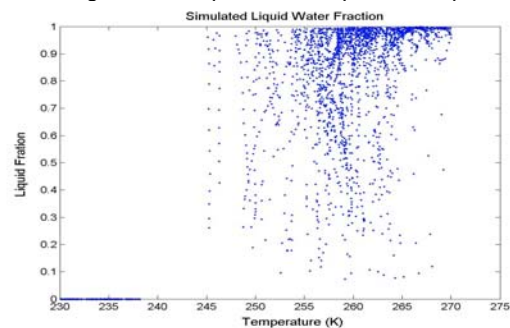


Figure 5 Model simulated liquid water fraction with the original setup

### 3.2 SENSITIVITY SIMULATION

The results in section 3.1 showed that the ice formation process is not efficient enough in the model. Figure 5 suggests that the temperature of homogeneous ice formation may be a crucial parameter that influences the ice formation. According to aircraft observation as shown in figure 2, we increase this temperature by 10°C to -25 °C. Sensitivity studies also show that the threshold of ice water content at which the Bergeron-Findeisen process starts and the threshold relative humidity used in the cloud scheme for calculating cloud cover and cloud water content could influence the SCM simulation significantly. In this sensitive study, we set them equal to  $IWC_{crit}=1$  mg/kg and  $RH_c=75\%$ , respectively. With these parameters the simulated cloud properties are shown in plate 3 and figures 6-8.

The cloud cover has improved significantly (plate 3), it now agrees well with the observations. The ice and liquid water content and liquid water fraction also agree better with the observations as shown in figures 6- 8.

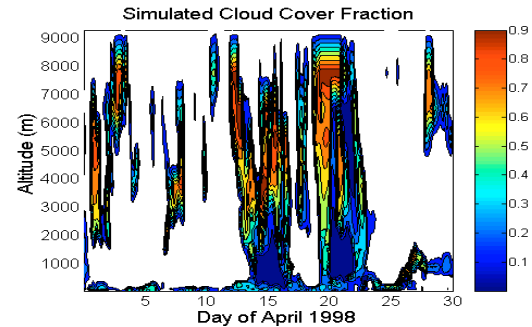


Plate 3 Simulated cloud cover with optimum parameters

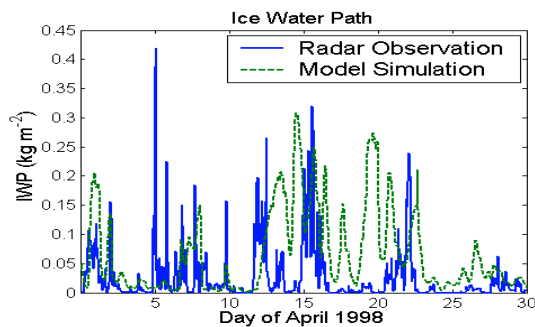


Figure 6 Comparison of ice water path

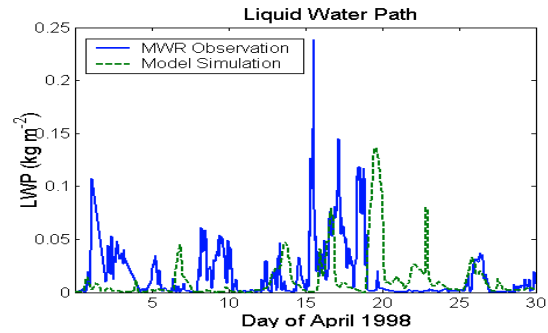


Figure 7 Comparison of liquid water path

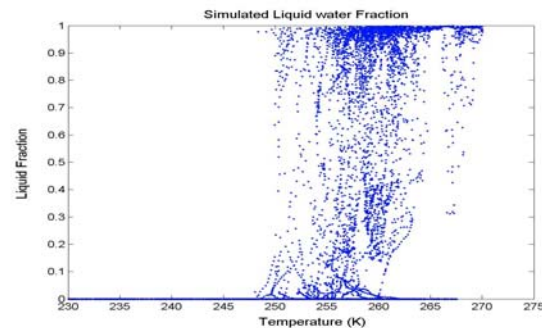


Figure 8 Simulated liquid water fraction with optimum parameters

### 3.3 IMPACT OF AEROSOL ON CLOUD PROPERTIES

In the SCM, prognostic equations of the cloud droplet and ice crystal number concentration are solved. Cloud droplet number concentration is calculated from the aerosol number concentration and vertical velocity [Lohmann et al, 1999]. In the previous experiments, we prescribed cloud droplet number as a function of height,  $220 \text{ cm}^{-3}$  near the surface decreasing to  $50 \text{ cm}^{-3}$  in the free troposphere. In this section we use the observed aerosol for the formation of cloud droplets to test the aerosol impact on cloud properties. The profile of aerosol number concentration at the model levels averaged over the 18 aircraft flights is shown in figure 9. The aerosol number concentration decreases from about  $230 \text{ cm}^{-3}$  near the surface to  $100 \text{ cm}^{-3}$  at 1000m, then increases with the height and arrives the maximum of  $300 \text{ cm}^{-3}$  at around 4500m, above which it decrease rapidly.

Using the observed aerosol number concentration to predict cloud droplet number concentration, the model predicts fewer clouds than observed below 2500m (plate 4). There is a significant

improvement for precipitation, although the precipitation is still less than observed (figure 10). However, the LWP has decreased in worse agreement with observations (not shown).

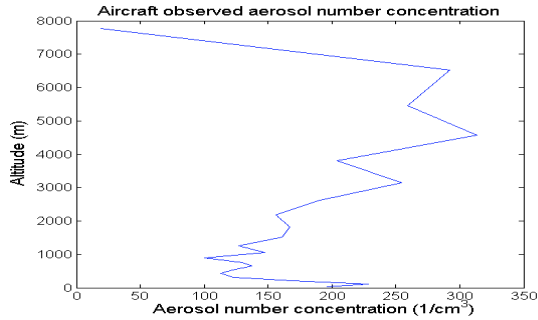


Figure 9 Aircraft observed profile of aerosol number

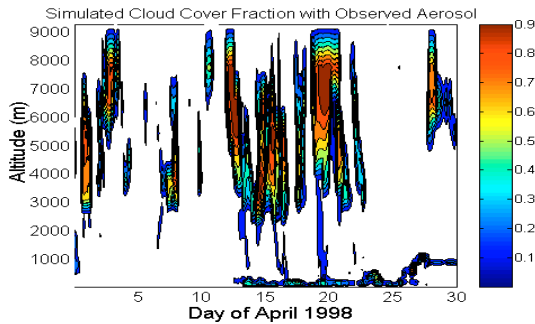


Plate 4 Simulated cloud cover by using the observed aerosol for the formation of cloud droplet

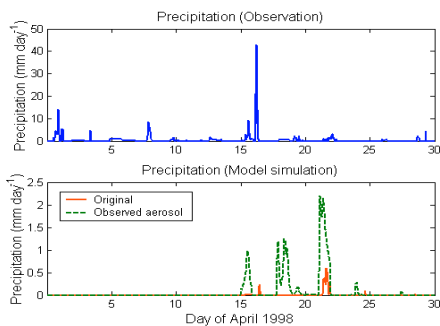


Figure 10 Comparison of precipitation

### 3.4 INTRODUCTION OF A PHYSICALLY BASED CONDENSATION/DEPOSITION RATE PARAMETERIZATION

In the statistical cloud scheme, the condensed (deposited) water content is calculated according to the assumption that sufficient condensation nuclei are present to remove any supersaturation. In the real atmosphere, however, condensation nuclei could be too limited to deplete the supersaturation within one time step. Therefore we introduced a

physically based condensation/deposition rate in the model following Rogers and Yau (1989):

$$\frac{dM}{dt} = \frac{4\pi C(S-1)}{\left[ \left( \frac{L}{R_v T} - 1 \right) \frac{L}{KT} + \frac{R_v T}{e_s(T)D} \right]} \quad (1)$$

Where  $M$  is cloud droplet/ ice crystal mass,  $S$  is the ambient saturation ratio,  $L$  is the latent heat of evaporation/sublimation,  $R_v$  is the individual constant of water vapor,  $T$  is the temperature,  $e_s$  is the equilibrium vapor pressure at temperature  $T$ ,  $K$  is the coefficient of thermal conductivity of air and  $D$  is the coefficient of diffusion of water vapor in air,  $C$  is the radius/capacitance of the cloud droplet/ice crystal.

Besides cloud droplets, three types of ice crystals are considered in the model: columns, plates, and dendrites. Compared with the original method, the new rate has very little impact on LWP, IWP, liquid water fraction and precipitation, it only redistributes the clouds cover a little (not shown). Similar results were obtained by Kain and Sednev [1996] when they used a 2-D ensemble model to simulate the precipitation event. The new condensation (deposition) rate, however, depends on other prognostic parameterizations such as the cloud droplet (ice crystal) number concentration whose impact will be studied in future.

### 4. CONCLUSION

Results from this study show that, with the proper parameters, the SCM can simulate the cloud properties well in the Arctic spring. When the observed aerosol was used to calculate the cloud droplet number concentration, it improves the precipitation, however the boundary layer clouds are shorter lived than observed. The new physically based condensation/deposition rate does not change the cloud properties much. The impact of aerosol on cloud properties and the new condensation (deposition) rate will be studied further in future.

### ACKNOWLEDGEMENT:

This research is supported by the National Science and Research Council of Canada (NSERC) and the Canadian Foundation for Climate and Atmospheric Science (CFCAS). We

thank Christian Jakob and his coworkers at ECMWF for producing the ECMWF column dataset for SHEBA, Mathew D. Shupe, Janet Intrieri, Taneil Uttal and their coworkers at NOAA/ETL for providing the radar and lidar datasets, Bing Lin and Alice Fan for the microwave radiometer data and Faisal Boudala, George A. Issac and their coworkers for providing the aircraft data.

## REFERENCES:

- Bretherton, C. S., S. R. de Roode, C. Jakob, E. L. Andreas, J. Intrieri, R. E. Moritz, and P. O. G. Persson, 2002: A comparison of the ECMWF forecast model with observations over the annual cycle at SHEBA. *J. Geophys. Res.*, submitted.
- Curry, J.A., and Coauthors, 2000: Fire Arctic Cloud Experiment, *Bull. Amer. Meteor. Soc.*, 81, 5-29.
- Curry, J.A., W.B. Rossow, D. Randall, and J. L. Schramm, 1996: Overview of Arctic cloud and radiation characteristics, *J. Clim.*, 9, 1731-1764.
- Ghan, S., and Coauthors, 2000: A comparison of single column model simulation of summertime midlatitude continental convection, *J. Geophys. Res.*, 105, 2091-2124.
- Intrieri, J.M., M. D. Shupe, T. Uttal, and B. J. Mccary, 2002: An annual cycle of Arctic cloud characteristics observed by radar and lidar at SHEBA, *J. Geophys. Res.*, submitted
- Khain, A. P., I. Sednev, 1996: Simulation of precipitation formation in the eastern Mediterranean coastal zone using a spectral microphysics cloud ensemble model, *Atmos. Res.*, 43, 77-110.
- Korolev, A. V., G. A. Isaac, and J. Hallett, 1999: Ice particle habits in Arctic clouds, *Geophys. Res. Lett.*, 26, 1299-1302.
- Lin, B., P. Minnis, A. Fan, J. A. Curry, and H. Gerber, 2001: Comparison of cloud liquid water paths derived from in situ and microwave radiometer data taken during the SHEBA/FIREACE, *Geophys. Res. Lett.*, 28, 975-978.
- Lohmann, U., N. McFarlane, L. Levkov, K. Abdella, F. Albers, 1999: Comparing different cloud schemes of a single column model by using mesoscale forcing and nudging technique, *J. Climate*, 12, 438-461.
- Persson, P. O. G., C. W. Fairall, E. L. Andreas, and P. S. Guest, 2002: Measurements of the meteorological conditions and surface energy budget near the atmospheric surface flux group tower at SHEBA, *J. Geophys. Res.*, submitted.
- Randall, D., and Coauthors, 1998: Status of and outlook for large-scale modeling of atmosphere-ice-ocean interaction in the Arctic, *Bull. Amer. Meteor. Soc.*, 79, 197-219
- Rogers, R. R., M. K. Yau, 1989: A short course of cloud physics, pregamon, Oxford
- Shupe, M.D., T. Uttal, S.Y. Matrosov, A.S. Frish, 2001: Cloud water contents and hydrometeor sizes during the FIRE Arctic clouds experiment, *J. Geophys. Res.*, 106, 15015-15028.
- Smith, R. N., 1990: A scheme for predicting layer clouds and their water content in a general circulation model, *Quart. J. Roy. Meteor. Soc.*, 116, 435-460.
- Sommeria, G., and J. W. Deardorff, 1977: Subgrid-scale condensation in models of nonprecipitating clouds, *J. Atmos. Sc.*, 34, 344-355.
- Uttal, T., and Coauthors, 2002: Surface Heat Budget of the Actic Ocean, *Bull. Amer. Meteor. Soc.*, 83, 255-275.